

Ag⁺–Keggin ion colloidal particles as novel templates for the growth of silver nanoparticle assemblies

Saikat Mandal, Debabrata Rautaray and Murali Sastry*

Materials Chemistry Division, National Chemical Laboratory, Pune 411 008, India.
 E-mail: sastry@ems.ncl.res.in; Fax: +91 20 5893952/5893044; Tel: +91 20 5893044

Received 18th June 2003, Accepted 17th September 2003

First published as an Advance Article on the web 14th October 2003

In the work reported in this paper, we demonstrate that Ag⁺–Keggin ion colloidal particles are excellent templates for the synthesis of organized assemblies of silver nanoparticles, wherein the Keggin ion host plays the role of a UV-switchable reducing agent. More specifically, we investigate the formation of aqueous colloidal particles of Ag⁺ ions complexed with phosphotungstate (PW₁₂O₄₀)³⁻ Keggin ions and show that they may be used as a new class of inorganic scaffolds in the synthesis of silver nanoparticle assemblies. The crystalline Keggin ion host may be reduced photochemically resulting in electron transfer to the entrapped silver ions and consequent formation of silver nanoparticle assemblies on the underlying colloidal particle surface. Treatment with alkali results in dissolution of the colloidal particle template leaving behind the silver nanoparticle network reasonably intact.

Introduction

There is increasing scientific interest in the growth of ordered two-dimensional (2D) and three-dimensional (3D) structures assembled from nanoparticles. Much of the work in this direction is stimulated by the potential use of ordered 2D and 3D nano/microstructures in advanced technologies such as photonics and plasmonics. The different techniques for the assembly of inorganic nanoparticles into materials with higher-order architecture are collectively termed *nanotectonics*. These include the shape-directed assembly¹ and programmed assembly² of nanoparticles comprising surface attached molecules, ligands, and recognition sites, as well as the formation of complex hybrid nanostructures by *in-situ* transformation of unstable nanoparticle-based precursors.³ The template-directed assembly includes the use of nanoparticles, which are spatially confined within organized interiors such as tobacco mosaic virus (TMV),⁴ carbon nanotubes,^{5,6} colloidal crystals,⁷ coated polymer beads⁸ and bacterial membranes.⁹ Synthesis of hierarchical ordered inorganic framework materials using different templates is of great importance because of their applications in catalysis,¹⁰ separation techniques¹¹ and materials chemistry. Over the last decade researchers have also used organic compounds as templates for the generation of inorganic structures and materials.^{12,13}

There is considerable current interest in the production of inorganic framework materials containing well defined pore networks such as microporous¹⁴ and mesoporous materials.¹⁵ In addition to organic templates, inorganic templates can also be used in the formation of inorganic materials.^{16–18} The process of transcription can be divided into several steps: first, an organic and inorganic template which consists of either preformed or self-assembled entities is brought into contact with an inorganic precursor or small particles of the actual inorganic material that will be formed. Deposition of the inorganic material on the inner or outer surface of the template will then result in the formation of an organic–inorganic or different inorganic hybrid material. The organic or inorganic template material can be removed by heat treatment,¹⁹ microwave irradiation,²⁰ washing with organic solvents,²¹ calcination²² or simple dissolution of the core particles,²³ which finally results in the formation of an inorganic material

possessing a morphology directly related to the organic or inorganic template.

Matišević and co-workers have shown that salts of Keggin ions with caesium²⁴ and thorium and zirconium²⁵ cations can form uniform micron-sized colloidal particles in aqueous medium. Keggin ions form a subset of polyoxometalates and have the general formula (XM₁₂O₄₀)⁽⁸⁻ⁿ⁾⁻, where ‘M’ stands for W or Mo and ‘X’ stands for heteroatoms such as P, Si, Ge with *n* being the valency of X.²⁶ The Keggin ions, accompanying cations and other components such as water are arranged in a well-defined secondary three-dimensional structure, the stability of which depends on the nature of counterions, amount of water, *etc.*²⁷ It is well known that polyoxometalates such as Keggin ions undergo stepwise multielectron redox processes without undergoing a structural change.²⁸ They may be reduced electrolytically, photochemically and with suitable reducing agents. Recently, Troupis, Hiskia and Papaconstantinou have shown that photochemically reduced polyoxometalates of the Keggin structure [(PW₁₂O₄₀)³⁻ and (SiW₁₂O₄₀)⁴⁻] when exposed to aqueous metal ions such as Ag⁺, AuCl₄⁻, Pd²⁺ and PtCl₆²⁻, resulted in the formation of the corresponding metal nanoparticles of reasonable monodispersity.²⁹ In this report, we show that crystalline, micron size colloidal particles of Ag⁺ ions complexed with phosphotungstate Keggin ions [(PW₁₂O₄₀)³⁻, PTA; step 1, Fig. 1A] may be used as templates for the *in-situ* synthesis of silver nanoparticles. UV-Irradiation of the colloidal particles results in photochemical reduction of the PTA anions and thereafter, electron transfer to the Ag⁺ ions from the electron-rich PTA ions and the consequent formation of silver nanoparticles (step 2, Fig. 1A). The crystalline PTA matrix thus acts as a UV-switchable reducing agent in the generation of metal nanoparticles within an open, inorganic framework. We observe assembly of the silver nanoparticles into interesting superstructures on the surface of the colloidal particles, possibly due to facile diffusion of the metal atoms within the channels of the open-framework Keggin particle. The silver nanoparticles are assembled predominantly on the edges of the Keggin ion framework thereby forming a 3-D superstructure. The Keggin ion template may be removed by simple dissolution in an alkaline medium leaving behind reasonably intact silver nanoparticle superstructures (step 3, Fig. 1A).

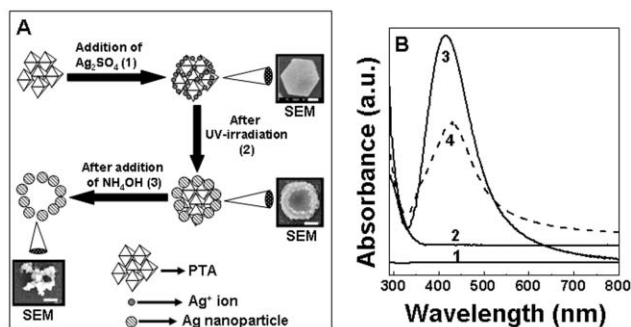


Fig. 1 (A) Scheme illustrating the various steps involved in the phosphotungstate ion-templated synthesis of silver nanoparticles (see text for details). (B) UV-vis spectra recorded from: curve 1 – aqueous mixture of 10^{-3} M phosphotungstic acid and 3×10^{-3} M Ag_2SO_4 before UV irradiation; curve 2 – UV-irradiated 3×10^{-3} M aqueous solution of Ag_2SO_4 in the absence of PTA; curve 3 – the solution shown as curve 1 after UV irradiation for 4 h; curve 4 – solution shown as curve 3 after addition of 10% NH_3 (aq) solution (see text for details).

Experimental

In a typical experiment, 10 ml of a 10^{-3} M aqueous deaerated solution of phosphotungstic acid [PTA, $\text{H}_3(\text{PW}_{12}\text{O}_{40})$], obtained from Aldrich as a powder and used as-received) was taken in a test tube along with 30 ml of a 10^{-3} M aqueous deaerated solution of Ag_2SO_4 and 2 ml of propan-2-ol (step 1, Fig. 1A). This mixture was irradiated by UV light (Pyrex filter, >280 nm, 450 W Hanovia medium pressure lamp) for 4 h (step 2, Fig. 1A). UV-Irradiation leads to the *in-situ* reduction of Ag^+ ions by the electron-rich $(\text{PW}_{12}\text{O}_{40})^{5-}$ ions (which are formed by the photochemical reduction of $(\text{PW}_{12}\text{O}_{40})^{3-}$ ions) and is clearly seen by the appearance of a brownish yellow color in the solution. 2 ml of 10% NH_3 (aq) was added to the UV-irradiated solution of Ag nano-PTA to dissolve the crystalline Keggin core template (step 3, Fig. 1A). UV-vis spectroscopy measurements of the Ag-PTA solution at different stages of treatment (steps 1, 2 and 3, Fig. 1A) were carried out on a Hewlett-Packard HP 8542A diode array spectrophotometer operated at a resolution of 2 nm. Samples for scanning electron microscopy (SEM) and energy dispersive analysis of X-rays (EDX) analysis from the Ag-PTA solutions at different stages of treatment (as indicated in Fig. 1A) were prepared by solution-casting films onto Si(111) wafers. SEM measurements were carried out on a Leica Stereoscan-440 scanning electron microscope equipped with a Phoenix EDX attachment. EDX spectra were recorded in the spot-profile mode by focusing the electron beam onto specific regions of the film.

Samples for TEM analysis were prepared by drop-coating films of the Ag-PTA solution after treatment with alkali (NH_4OH) solution (step 3, Fig. 1A) on carbon-coated copper TEM grids, allowing the grid to stand for 2 min following which the extra solution was removed using a blotting paper. The films of silver nanoparticles thus obtained were subjected to TEM analysis on a JEOL model 1200EX instrument operated at an accelerating voltage at 120 kV. X-Ray diffraction (XRD) analysis of drop-coated films of the Ag-PTA solution at different stages of chemical treatment on glass substrates were carried out on a Phillips PW 1830 instrument operating at a voltage of 40 kV and a current of 30 mA with $\text{Cu-K}\alpha$ radiation.

Results and discussion

Fig. 1B shows the UV-vis spectra of aqueous mixtures of 1×10^{-3} M PTA and 3×10^{-3} M Ag_2SO_4 solutions at different stages of treatment. Prior to UV-irradiation, it is observed that there is little absorption in the visible region of

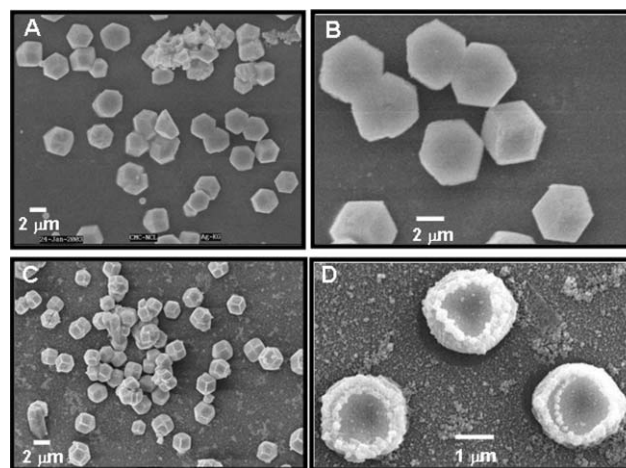


Fig. 2 (A) and (B) - Low and high magnification SEM images of PTA- Ag^+ ion solution before UV-irradiation, respectively. (C) and (D) - Low and high magnification SEM images of PTA- Ag^+ solution after UV-irradiation, respectively (see text for details).

the electromagnetic spectrum (curve 1, Fig. 1B, step 1, Fig. 1A). Fig. 2A and B show representative SEM images recorded at different magnifications from a drop-coated film of the aqueous mixture of PTA and silver sulfate on a Si (111) substrate. Densely populated colloidal particles of the Ag^+ -PTA complex are seen on the surface of the substrate. The particles are extremely uniform in size (average size ~ 2.3 μm) and exhibit well-defined morphology that appears to be predominantly rhombohedral (Fig. 2B). The XRD pattern recorded from this drop-coated film is shown as curve 1, Fig. 3A. A number of sharp Bragg reflections are observed that are characteristic of the Keggin structure.^{24,25} Thus, the Ag^+ -PTA colloidal particles observed in the SEM images (Fig. 2A and B) are crystalline with no discernible disturbance to the Keggin structure.

The UV-vis absorption spectrum recorded after UV-irradiation of the 10^{-3} M PTA/ 3×10^{-3} M Ag_2SO_4 aqueous solution for 4 h is shown as curve 3 in Fig. 1B (step 2, Fig. 1A). A prominent and sharp absorption band is observed to form at 430 nm. This absorption band is characteristic of silver nanoparticles and arises due to excitation of surface plasmon vibrations in the nanoparticles. Representative SEM pictures recorded from drop-coated films of this UV-irradiated solution on a Si(111) wafer are shown in Fig. 2C and D at different magnifications. Comparison of the low magnification images recorded before (Fig. 2A) and after UV-irradiation indicates an interesting increase in contrast of the edges of the nanoparticles

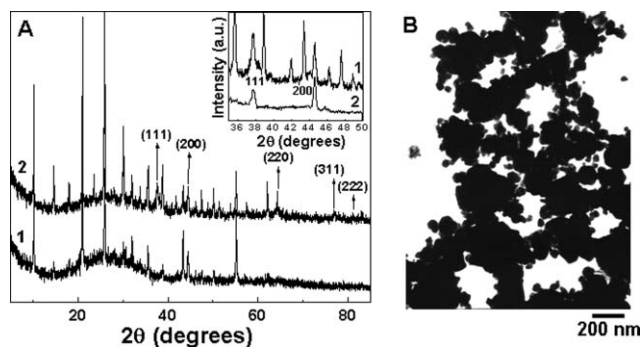


Fig. 3 (A) XRD patterns recorded from drop-coated films on glass substrates of the PTA- Ag^+ ion solution before (curve 1) and after UV-irradiation (curve 2). The inset of this figure shows a magnified view of the XRD spectra of the UV-irradiated Ag nano-PTA solution before (curve 1) and after alkali treatment (curve 2) (see text for details). (B) TEM picture of the UV-irradiated PTA- Ag nanoparticle solution after alkali treatment.

relative to the remainder of the particle surface after UV-irradiation. This is much more clearly seen in the higher magnification SEM image of some of the particles (Fig. 2D) where the presence of spherical silver nanoparticles arranged along the edges in a quasi-circular fashion is observed. The silver particles range in size from 80 to 150 nm and are thus, not monodisperse. The silver nanoparticles formed by electron transfer from the UV-irradiated Keggin ions to the Ag^+ ions are preferentially assembled at the edges of the colloidal crystals. Thus, the high energy edge regions of the colloidal particles play a crucial role in assembling the *in-situ* formed silver nanoparticles. It is possible that the Ag^+ ions within the colloidal crystals are reduced by direct exposure to UV-irradiation and not due to electron transfer from photochemically excited PTA ions. In order to preclude this possibility, a control experiment was performed wherein a 3×10^{-3} M aqueous solution of Ag_2SO_4 was irradiated by UV light for 4 h without PTA ions. The UV-vis absorption spectrum recorded from this solution is shown as curve 2 in Fig. 1B. There is no evidence of absorption in the 400–450 nm window, clearly showing the silver nanoparticles are formed due to the reduced Keggin ions, and not due to direct UV-reduction of the Ag^+ ions in the colloidal particles.

A detailed chemical analysis of the surface of the colloidal particles after formation of silver nanoparticles as described above was performed using spot-profile EDX. Fig. 4A shows an enlarged SEM image of one of the colloidal particles decorated with silver nanoparticles and spot-profile EDX spectra from specific regions of the particle surface (Fig. 4B and C). The bright regions populated by the particles are clearly rich in silver (Fig. 4A) while away from the particle edge, the silver signal is relatively weak and is accompanied by a strong W signal. This result clearly shows that the silver particles are formed at the edges of the colloidal particle and is accompanied by depletion from other regions of the particle. We believe that this occurs by diffusion of silver atoms to the surface *via* channels in the open Keggin structure framework and aggregation at the edges leading to the characteristic assembly of the silver nanoparticles observed.

The XRD pattern recorded from a drop-coated film of the UV-irradiated sample on a glass substrate is shown as curve 2 in Fig. 3A. The Bragg reflections corresponding to the Keggin structure are intact indicating that the formation of silver nanoparticles on the Keggin colloidal particle template does not disrupt the Keggin structure. The inset of Fig. 3A shows

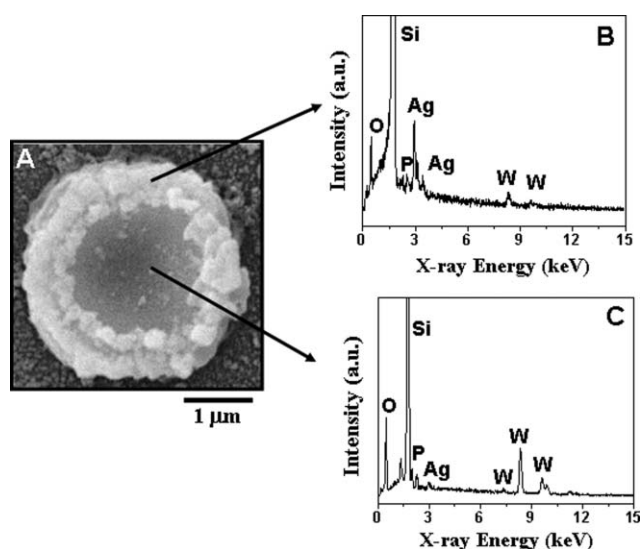


Fig. 4 (A) SEM image of a colloidal particle in a drop-coated film on a Si(111) substrate from PTA- Ag^+ solution after UV-irradiation. The accompanying EDX profiles (B and C) have been recorded from the regions indicated by arrows in the SEM picture (see text for details).

the XRD pattern obtained from the Ag^+ -PTA colloidal particles after UV-irradiation (curve 1) in the region of the principal Bragg reflections of silver. The (111) and (200) Bragg reflections of fcc silver are clearly observed along with some of the peaks of the Keggin structure. Relative to the Keggin Bragg reflections, the silver peaks are broad indicating that the silver particles are quite small. It is possible that the 80–150 nm size silver nanoparticles observed in the SEM images are composed of smaller silver nanoparticles separated by Keggin ions. This is purely speculative since we have not been able to image the individual silver nanoparticles in the assembly.

The UV-vis spectrum of the Ag nano-PTA particles in solution after alkali treatment is shown as curve 4, Fig. 1B (step 3, Fig. 1A). A slight broadening of the absorption band is observed with the absorption maximum remaining unchanged at 430 nm. Though the slight broadening of the surface plasmon absorption band indicates some degree of aggregation of the silver nanoparticles consequent to removal of the PTA scaffold, we did not observe any long-term instability in the solution over weeks of storage. In an alkaline medium, it is known that phosphotungstate ions dissociate into phosphate (PO_4^{3-}) and tungstate (WO_4^{2-}) ions.³⁰ It is therefore probable that such phosphate and tungstate ions bind to the silver nanoparticles and stabilize them against aggregation. The presence of silver nanoparticle surface-bound decomposition products is substantiated by SEM/EDX analysis of the alkali-treated Ag nano-PTA solution as described below.

Fig. 5A shows a high magnification electron microscopy image recorded from a drop-coated film of the silver nanoparticle structures after alkali treatment of UV-irradiated Ag nano-PTA solution. The image clearly shows that the Keggin colloidal particle scaffold has dissolved leaving behind the silver nanoparticle assembly reasonably intact. The removal of the Keggin scaffold is clearly shown in the spot-profile EDX analysis of the gap region (Fig. 5C) – there is no evidence of either Ag or tungsten and only peaks characteristic of the Si substrate are observed. It is interesting to note that there is very little spillover of the silver nanoparticles into the core of the template indicating a high degree of fidelity to the PTA template for assembling the inorganic materials. The EDX spectrum from the bright regions populated by the particles (Fig. 5B) shows that it is composed primarily of silver and a small percentage of tungsten and phosphorus. Removal of the PTA scaffold does lead to some aggregation of the smaller silver nanoparticles and would thus explain the broadening of UV-vis spectrum observed after alkali dissolution

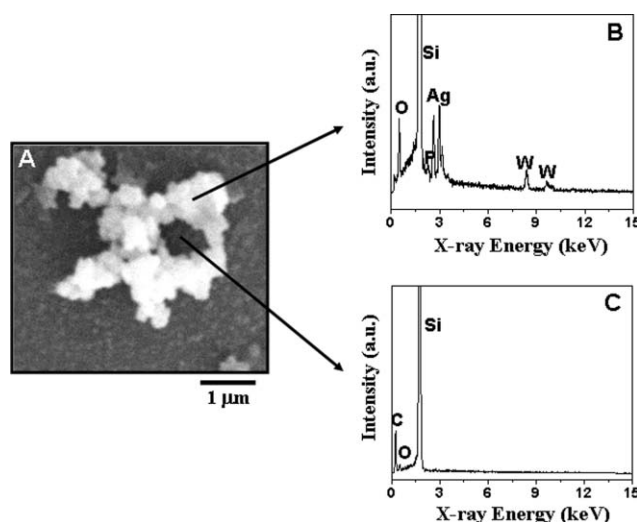


Fig. 5 (A) SEM image of a drop-coated film on a Si(111) substrate from a UV-irradiated PTA- Ag^+ solution after alkali treatment. The accompanying EDX profiles (B and C) have been recorded from the regions indicated by arrows in the SEM picture (see text for details).

of the Keggin scaffold (Fig. 1B, curve 4). The presence of W and P signals, thus clearly indicates the presence of the tungstate (WO_4^{2-}) and phosphate (PO_4^{3-}) decomposition products on the surface of the silver nanoparticles, that stabilize the smaller silver nanoparticles in the aggregated structures. The surface capping also prevents uncontrolled aggregation of the silver nanoparticle super-assemblies in solution and would explain the long-term stability of the alkali-treated Ag nano-PTA solutions.

The XRD pattern recorded from a drop-coated film of the Ag nano-PTA solution after alkali dissolution of the Keggin scaffold is shown in the inset of Fig. 4A (curve 2). It is clear that the Bragg reflections of the Keggin scaffold have disappeared leaving behind just the Bragg reflections of the Ag nanoparticle assembly. The fact that the (200) Bragg reflection is more intense than the (111) reflection indicates oriented growth of the silver nanoparticles on the Keggin scaffold.

An attempt was made to resolve the silver particles into smaller silver nanoparticles by TEM and a representative image of the silver nanoparticle assembly after alkali dissolution of the Keggin scaffold is shown in Fig. 3B. As in the case of the SEM images, regular and well-defined pores are observed where the Keggin scaffold originally existed. The silver particles themselves are quite large and are possibly arranged in a three-dimensional fashion making it difficult to image possible smaller subunits in the transmission mode.

In conclusion, it has been shown that highly organized assemblies of silver nanoparticles can be formed by using crystalline Ag^+ -Keggin ion colloidal particles as precursors. The salient feature of this approach is that the Keggin ions play a multifunctional role – they provide the crystalline framework to support the metal cations and also participate in the reduction of the metal ions without disruption to the well-defined Keggin structure. The possibility of using the Keggin framework as a UV-switchable reducing matrix is exciting and may be extended to the creation of other highly organized hybrid (nano)inorganic structures with possible applications in catalysis and novel optical materials.

Acknowledgements

S. M. and D. R. thank the University Grants Commission (UGC) and Indo-French Center for the Promotion of Advanced Scientific Research (IFCPAR), New Delhi for financial support. We are grateful to Dr Ganesh Pandey, Organic Chemistry (Synthesis) Division, NCL Pune for permission to use his UV-irradiation apparatus. TEM and SEM analysis by Ms Renu Pasricha and Dr Sudhakar Sainkar, Centre for Materials Characterization, NCL Pune is gratefully acknowledged.

References

- 1 M. Li, H. Schnablegger and S. Mann, *Nature*, 1999, **402**, 393.
- 2 (a) C. A. Mirkin, R. L. Letsinger, R. C. Mucic and J. J. Storhoff, *Nature*, 1996, **382**, 607; (b) P. Alivasatos, K. P. Johnsson, X. Peng, T. E. Wilson, C. J. Loweth, M. Bruchez and P. G. Schultz, *Nature*, 1996, **382**, 609; (c) W. Shenton, S. A. Davis and S. Mann, *Adv. Mater.*, 1999, **11**, 449; (d) S. Connolly and D. Fitzmaurice, *Adv. Mater.*, 1999, **11**, 1202.
- 3 M. Li and S. Mann, *Langmuir*, 2000, **16**, 7088.
- 4 W. Shenton, T. Douglas, M. Young, G. Stubbs and S. Mann, *Adv. Mater.*, 1999, **11**, 253.
- 5 G. Che, B. B. Lakshmi, C. R. Martin and E. R. Fisher, *Langmuir*, 1999, **15**, 750.
- 6 B. Xue, P. Chen, Q. Hong, J. Lin and K. L. Tan, *J. Mater. Chem.*, 2001, **11**, 2378.
- 7 S. A. Davis, H. M. Patel, E. L. Mayes, N. H. Mendelson, G. Franco and S. Mann, *Chem. Mater.*, 1998, **10**, 2516.
- 8 F. Caruso, H. Lichtenfeld, M. Giersig and H. Möhwald, *J. Am. Chem. Soc.*, 1998, **120**, 8523.
- 9 S. R. Hall, W. Shenton, H. Engelhardt and S. Mann, *Chem. Phys. Chem.*, 2001, **3**, 184.
- 10 P. T. Tanev, M. Chibwe and T. J. Pinnavaia, *Nature*, 1994, **368**, 321.
- 11 Y. N. Jun, D. M. Dabbs, I. A. Aksay and S. Erramilli, *Langmuir*, 1994, **10**, 3377.
- 12 N. K. Raman, M. T. Anderson and C. J. Brinker, *Chem. Mater.*, 1996, **8**, 1682.
- 13 S. Mann, S. L. Burkett, S. A. Davis, C. E. Fowler, N. H. Mendelson, S. D. Sims, D. Walsh and N. T. Whilton, *Chem. Mater.*, 1997, **9**, 2300.
- 14 (a) T. Bein, *Chem. Mater.*, 1996, **8**, 1636; (b) M. E. Davis, *Chem. Eur. J.*, 1997, **3**, 1745.
- 15 C. G. Goltner and M. Antonietti, *Adv. Mater.*, 1997, **9**, 431.
- 16 P. A. Buining, B. M. Humbel, A. P. Philipse and A. J. Verkleij, *Langmuir*, 1997, **13**, 3921.
- 17 M. Giersig, T. Ung, L. M. Liz-Morzan and P. Mulvaney, *Adv. Mater.*, 1997, **9**, 570.
- 18 S. Santra, R. Tapeç, N. Theodoropoulou, J. Dobson, A. Hebart and W. Tan, *Langmuir*, 2001, **17**, 2900.
- 19 N. Kawahashi and E. Matijevic, *J. Colloid Interface Sci.*, 1991, **143**, 103.
- 20 K. W. Gallis and C. C. Landry, *Adv. Mater.*, 2001, **13**, 23.
- 21 Y. Lu, Y. Yin and Y. Xia, *Adv. Mater.*, 2001, **13**, 271.
- 22 F. Caruso, M. Spasova, A. Susha, M. Giersig and R. A. Caruso, *Chem. Mater.*, 2001, **13**, 109.
- 23 F. Caruso, *Chem. Eur. J.*, 2000, **6**, 413.
- 24 L. A. Perez-Maqueda and E. Matijevic, *Chem. Mater.*, 1998, **10**, 1430.
- 25 A. Koliadima, L. A. Pérez-Maqueda and E. Matijevic, *Langmuir*, 1997, **13**, 3733.
- 26 J. A. Huheey, *Inorganic Chemistry*, 3rd edn., Harper and Row, New York, 1983, p. 698.
- 27 M. Misono, *Mater. Chem. Phys.*, 1987, **17**, 103.
- 28 (a) M. T. Pope and A. Muller, *Angew. Chem., Int. Ed. Engl.*, 1991, **30**, 34; (b) V. Kogan, Z. Izenshtat and R. Neumann, *Angew. Chem., Int. Ed.*, 1999, **38**, 3331.
- 29 A. Troupis, A. Hiskia and E. Papaconstantinou, *Angew. Chem., Int. Ed.*, 2002, **41**, 1911.
- 30 F. A. Cotton and G. Wilkinson, *Advanced Inorganic Chemistry*, 5th edn., John Wiley and Sons, New York, 1988, p. 817.